INVITED PAPER *Special Section on Recent Progress in Antennas and Propagation in Conjunction with Main Topics of ISAP2016*

An Overview of China Millimeter-Wave Multiple Gigabit Wireless Local Area Network System

Wei HONG[†a)], Shiwen HE[†b)], Haiming WANG[†c)], Guangqi YANG[†d)], Yongming HUANG[†e)], Jixing CHEN[†f)], Jianyi ZHOU[†g)], Xiaowei ZHU[†h)], Nianzhu ZHANG[†i)], Jianfeng ZHAI[†j)], Luxi YANG[†k)], Zhihao JIANG[†l)], *and* Chao YU[†m)], *Nonmembers*

SUMMARY This paper presents an overview of the advance of the China millimeter-wave multiple gigabit (CMMG) wireless local area network (WLAN) system which operates in the 45 GHz frequency band. The CMMG WLAN system adopts the multiple antennas technologies to support data rate up to 15 Gbps. During the progress of CMMG WLAN standardization, some new key technologies were introduced to adapt the millimeter-wave characteristic, including the usage of the zero correlation zone (ZCZ) sequence, a novel lower density parity check code (LDPC)-based packet encoding, and multiple input multiple output (MIMO) single carrier transmission. Extensive numerical results and system prototype test are also given to validate the performance of the technologies adopted by CMMG WLAN system.

key words: *millimeter wave communications, wireless local area network (WLAN), zero correlation zone, single carrier, MIMO*

1. Introduction

Since the world's first 4G (LTE: Long Term Evolution) pre-commercial network was launched by the Swedish mobile network operator (MNO) Telia on May 27, 2009, the deployment of 4G networks has been accelerated all over the world. Meanwhile, the rapid adoption of smart phones has triggered the Internet paradigm shift, from desktop to handhold. As a result, the mobile data traffic also increases explosively with conservative estimates ranging from 40% to 70% year-by-year [1]–[3]. The incredible growth implies that the wireless network in 2020 should be capable of providing 1000 times more capacity and 10 ∼ 100 times more connections compared with the current network.

To meet these requirements, there has been growing interest in millimeter wave (mmWave) communications due to the huge bandwidth in the mmWave band from 30 GHz to 300 GHz [4]–[11]. The available spectrum at these higher frequencies can be easily 200 times greater than all cellular allocations with sub-6 GHz. Moreover, the very small wavelengths of mmWave signals combined with the rapid advances of low-power complementary metal-oxide-semiconductor (CMOS) radio frequency integration circuit (IC) solutions enable large numbers of miniaturized antennas and mmWave front-ends to be placed in a small space [12]–[16]. As a consequence, mmWave wireless communication becomes one of the most promising candidates for future wireless communication networks [17]–[28].

Recently, many communication technology standards on mmWave wireless communications have been formulated, including the IEEE 802.15.3c [29] wireless personal area network (WPAN), wireless high definition (WiHD) [30], European computer manufacturers association (ECMA) [31], IEEE 802.11ad wireless local area network (WLAN) [32], and China millimeter-wave multiple gigabit (CMMG) wireless local area networks [33]. The emergence of these new standards have further validated the feasibility of indoor implementation of mmWave wireless communications [34], [35].

IEEE 802.15.3 Task Group 3c (TG3c) was formed in March 2005 with aiming to developing an mmWave-based alternative physical layer (PHY) for the existing 802.15.3 WPAN Standard 802.15.3-2003. This mmWave WPAN standard is defined to operate in the 57 – 66 GHz range. IEEE 802.15.3c-2009, which was published on September 11, 2009, allows very high data rate, short range (10 m) for applications including high speed internet access, streaming content download (video on demand, HDTV, home theater, etc.), real time streaming and wireless data bus for cable replacement. A total of three PHY modes were defined in the standard [29]:

- Single carrier (SC) mode (up to 5.3 Gbit/s)
- High speed interface (HSI) mode (single carrier, up to 5 Gbit/s)
- Audio/visual (AV) mode (OFDM, up to 3.8 Gbit/s).

The WiHD specification is a high definition digital interface operating in the 60 GHz frequency radio band [30]. It allows either lightly compressed or uncompressed digital transmission of high-definition video and audio and data signals. The standard ECMA specifies a PHY, a media access control (MAC), and an High Definition Multimedia Inter-

Manuscript received February 27, 2017.
Manuscript revised June 19, 2017.
Manuscript publicized August 22, 2017.

[†]The authors are with the School of Information Science and Engineering, Southeast University, Nanjing 210096, China.
a) E-mail: weihong@seu.edu.cn
b) E-mail: shiwenhe@seu.edu.cn
c) E-mail: hmwang@seu.edu.cn
d) E-mail: gq.yang@seu.edu.cn
e) E-mail: huangym@seu.edu.cn
f) E-mail: jxchen@seu.edu.cn
g) E-mail: jyzhou@seu.edu.cn
h) E-mail: xwzhu@seu.edu.cn
i) E-mail: nzzhang@seu.edu.cn
j) E-mail: zhaijianfeng@seu.edu.cn
k) E-mail: lxyang@seu.edu.cn
l) E-mail: zhihao.jiang@seu.edu.cn
m) E-mail: chao.yu@seu.edu.cn

DOI: 10.1587/transcom.2017ISI0004

face (HDMI) protocol adaptation layer (PAL) [31].

The IEEE 802.11 standard for wireless LANs (WLANs) has many versions including 11b, 11a, 11g, 11n, 11ac, and 11ad. The 11b/g/n standards operate in the 2.4-GHz band. The 11a/ac/n standards operate in the 5-GHz band, and the 11ad standard targets the 60-GHz band. All share a similar MAC layer to provide interoperability. The IEEE 802.11ad working group developed the 11ad standard with input from the Wireless Gigabit Alliance (WiGig). The 11ad standard divides the 60-GHz band into four 2.16-GHz wide channels and supports data rates up to 8.085 Gbps [36].

The purpose of this paper is to review the recent advances and results on the China millimeter-wave multiple gigabit (CMMG) WLAN system and standardization, which is named as IEEE 802.11aj. IEEE 802.11aj is a wireless networking standard in the 802.11 family, developed in the IEEE Standards Association process, providing high-throughput WLANs [37]. IEEE 802.11aj system operates in the 45-GHz frequency band named as CMMG WLAN standard and in the 60-GHz frequency band called as China directional multiple gigabit (CDMG) WLAN standard, respectively. CMMG adopts (digital-analog hybrid) MIMO structure to simultaneously achieve the diversity-multiplexing gain with theoretical peak throughput up to 15 Gbps via transmitting more spatial streams (up to four) [38]. Except for exploiting the antenna array gain to compensate the large path-loss, a novel robust low density parity checking (LDPC) codes based packet encoding was adopted to improve the code gain with up to 0.2-0.5 dB in CMMG [39].

The rest of this paper is organized as follows. The progress of CMMG WLAN standard is briefly introduced in Sect. 2. Sect. 3 introduces the channelization of CMMG WLAN standard, followed by the introduction of the preamble in Sect. 4. A novel LDPC-based packet encoding scheme is introduced in Sect. 5. Section 6 introduces the detail of the basic architecture of the CMMG WLAN standard and the corresponding key technologies. The performance evaluation is given in Sect. 7.

2. Progress of CMMG WLAN Standard

A new study group SG5 with the aim to researching the feasibility of 45 GHz frequency band for WLAN application was setup in Chinese Wireless Personal Access Network (CWPAN) Standard Working group in 2010. The first author from Southeast University was the chair of the SG5.

In January 2012, a new study group (SG) IEEE 802.11 cmmw was setup [37], [40], [41] in IEEE 802.11 working group. The main task of this group is to investigate the possibility of using the mmWave frequency bands including the 59 – 64 GHz and the 45 GHz frequency band to achieve multi-Gbps wireless transmission with lower power in China. The task group TGaj was formally established in September 2012. Figure 1 illustrates the progress of CMMG WLAN standard, which operates on the 45 GHz frequency band. Up to now, the letter ballots of CMMG WLAN standard has basically finished. According to the time line of the CMMG WLAN standard, in March 2017, the task group will launch the sponsor ballots of CMMG WLAN standard. The task group plans to formally publish the CMMG WLAN standard in July 2017.

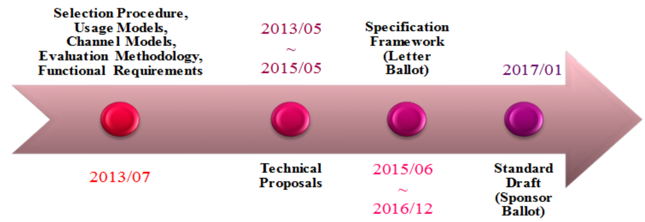

Fig. 1 Progress of CMMG WLAN standardization.

In what follows, we focus on introducing the key technologies adopted in CMMG WLAN standard. Due to the fact that the 45 GHz frequency band is a whole new frequency band for IEEE 802.11 standardization organization, coexistence problem need not to be considered. According to the project authorization request (PAR), a new physical (PHY) and an amendment of the media access control (MAC) should be defined to adopt the advantage of this new 45 GHz frequency band.

3. Channelization of CMMG WLAN Standard

In 2011, a series of application documents of the mmWave, especially for the 45 GHz, frequency band were submitted to the Radio Management Bureau of the Ministry of the Industry and Information Technology (MIIT) of the People's Re-public of China for the usage of the 45 GHz frequency band [41]. After multiple rounds of modification, the document named as "The usage of 40 – 50 GHz frequency band for mobile services in broadband wireless access systems" was published in the MIIT website [42], which was intended to ask for suggestions and comments in September 2013. The authorized frequency band that can be used for CMMG WLAN standard is 42.3 GHz to 47.0 GHz and 47.2 GHz to 48.4 GHz.

Taking the spectrum efficiency, the required peak rate, and the implementation complexity into account, IEEE 802.11aj CMMG task group, designed two kinds of channel bandwidth, i.e., 540 MHz and 1080 MHz, for the CMMG WLAN standard. Figure 2 illustrates the spectrum allocation and the channelization of the CMMG WLAN standard to adapt to different data rate requirements and hardware implementations. There are ten 540 MHz channels and five 1080 MHz channels. Note that there is 200 MHz frequency gap between 47.0 GHz and 47.2 GHz, which has been allocated for the amateur radio application. Compared to the frequency allocation at the 60 GHz for IEEE 802.11ad in China [32], as illustrated in Fig. 3 and Fig. 4, there are more separable channels in the CMMG WLAN standard, which facilitates the formation of mutually interference free basic service set (BBS) networks and enhance the user experiences. The main parameters of frequency band of the

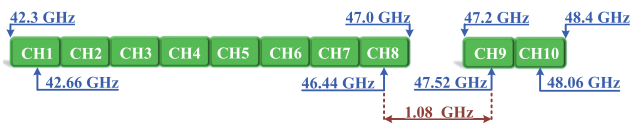

(a) Channelization for channel bandwidth 540 MHz

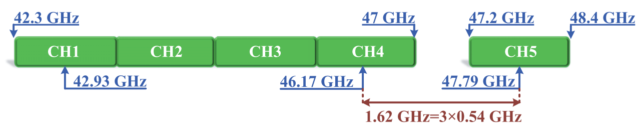

(b) Channelization for channel bandwidth 1080 MHz

Fig. 2 Channelization for CMMG WLAN communication standard.

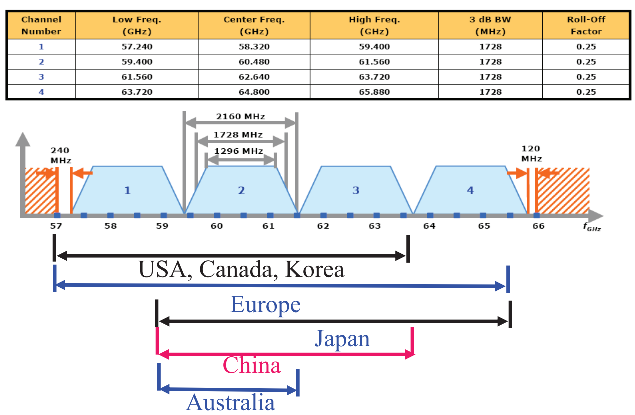

Fig. 3 Frequency allocation at 60 GHz frequency band for IEEE 802.11ad [43].

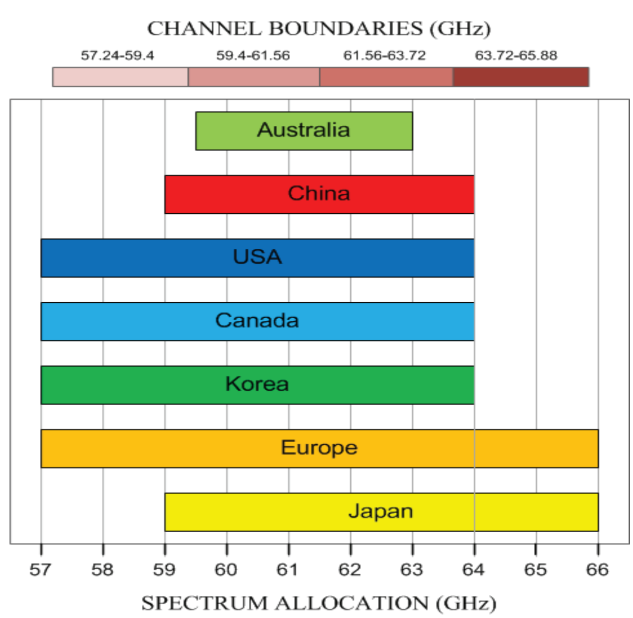

Fig. 4 Frequency allocation at 60 GHz frequency band for IEEE 802.11ad [43].

CMMG WLAN standard are listed in Table 1, where EIRP is the abbreviation of Equivalent Isotropic Radiated Power (EIRP).

Three different application scenarios including conference room, cubicle office, and living room, are defined in the usage scenarios document for CMMG WLAN standard [48]. A general structure of a channel model that takes account of the important properties of 45 GHz electromagnetic wave propagation was proposed in [47], [49].

Table 1 Main regulation parameters of CMMG WLAN communication system.

Item	Value
Frequency band (GHz)	42.3-47.0, 47.2-48.4
Bandwidth (MHz)	540, 1080
Frequency tolerance	100 ppm
Maximum transmit power at antenna port	20 dBm
Maximum EIRP	36 dBm

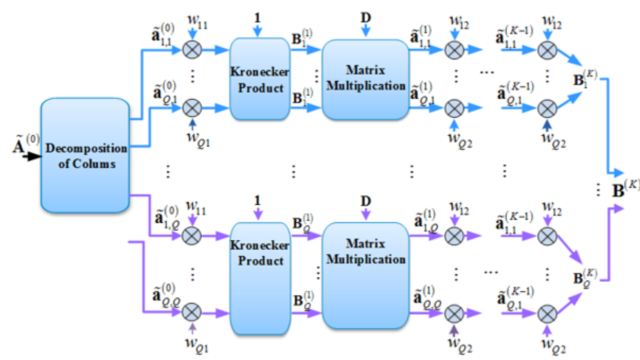

Fig. 5 Matrix factorized weighted construction method of ZCZ sequence.

4. Preamble Sequence of CMMG WLAN Standard

As we all know that in wireless communication systems, timing/frequency synchronization and channel estimation are two main tasks achieved by training signal in the receiver. Furthermore, accurate synchronization and channel estimation play important roles in improving the overall system performance. It also means that the design of the training sequence set, which is known to both transmitter and receiver, is a crucial problem. The zero correlation zone (ZCZ) sequence that is firstly introduced to enhance the robustness of synchronization in code division multiple access (CDMA) system [50], is adopted to be the short training field (STF) sequence and the channel estimation field (CEF) sequence in CMMG WLAN standard. CMMG task group adopted the matrix factorized weighted construction method to generate the ZCZ sequence set based on a base ZCZ sequence set, which has the shortest length with interleaving techniques [45], [46]. Figure 5 illustrates the details of the generation of the adopted ZCZ sequence.

In Fig. 5, $\widetilde{\boldsymbol{A}}^{(0)}$, $\widetilde{\boldsymbol{A}}^{(k)}$ and $\widetilde{\boldsymbol{B}}^{(k)}$ are defined as follows, respectively.

$$\widetilde{\boldsymbol{A}}^{(0)} = \begin{pmatrix} \widetilde{\boldsymbol{a}}^{(0)}_{1,1} & \cdots & \widetilde{\boldsymbol{a}}^{(0)}_{1,Q} \\ \vdots & \ddots & \vdots \\ \widetilde{\boldsymbol{a}}^{(0)}_{Q,1} & \cdots & \widetilde{\boldsymbol{a}}^{(0)}_{Q,Q} \end{pmatrix}$$

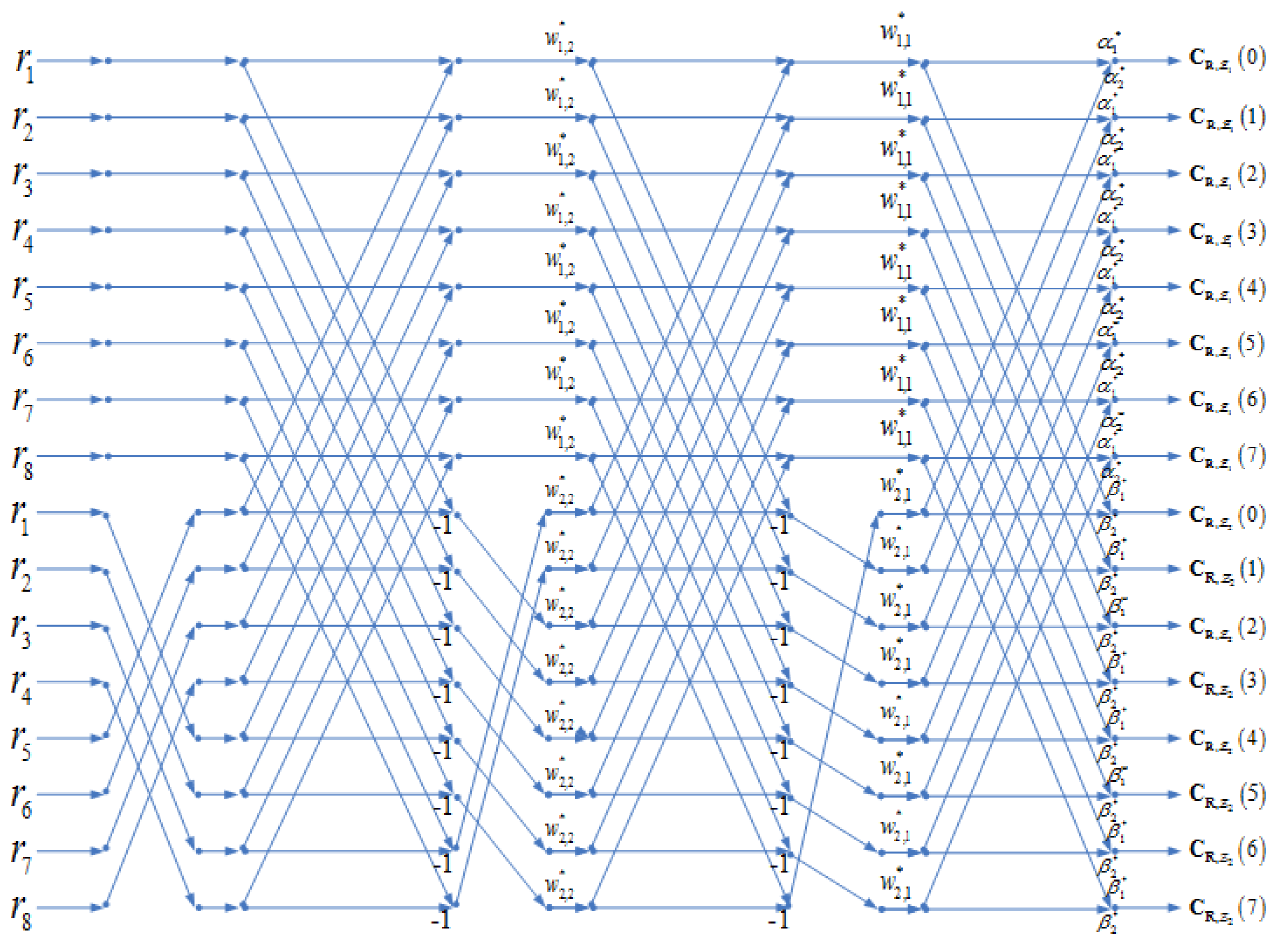

Fig. 6 Fast correlator of ZCZ.

$$\boldsymbol{B}^{(k)} = \begin{pmatrix} w_{1,k}\boldsymbol{I}_{Q^{k-1}L} & \cdots & \boldsymbol{0}_{Q^{k-1}L} \\ \vdots & \ddots & \vdots \\ \boldsymbol{0}_{Q^{k-1}L} & \cdots & w_{Q,k}\boldsymbol{I}_{Q^{k-1}L} \end{pmatrix} \widetilde{\boldsymbol{A}}^{(k-1)}$$

$$\widetilde{\boldsymbol{A}}^{(k)} = \boldsymbol{D}\left(\boldsymbol{1} \otimes \boldsymbol{B}^{(k)}\right)$$

$$\boldsymbol{D} = \begin{pmatrix} f_{1,1}\boldsymbol{I}_{Q^{k-1}L} & \cdots & \boldsymbol{0}_{Q^{k-1}L} \\ \vdots & \ddots & \vdots \\ \boldsymbol{0}_{Q^{k-1}L} & \cdots & f_{Q,Q}\boldsymbol{I}_{Q^{k-1}L} \end{pmatrix}$$

where L is the length of the initial sequence $\widetilde{\boldsymbol{a}}_{i,j}^{(0)}$, $i, j = 1, \cdots, Q$. Q denotes the number of the ZCZ sequences. $w_{i,j} \in \left\{\pm 1, \pm\sqrt{-1}\right\}$, $i = 1, \cdots, Q$, $j = 1, \cdots, K$ are elements of the weight matrix $\boldsymbol{W}$ of size $Q \times K$. $K \geq 2$ denotes the number of the iterations. $\boldsymbol{I}_{Q^{k-1}L}$ and $\boldsymbol{0}_{Q^{k-1}L}$ denote an $Q^{k-1}L \times Q^{k-1}L$ identity matrix and an $Q^{k-1}L \times Q^{k-1}L$ zero matrix, respectively. $Q^K L$ is the length of the ZCZ sequence. $f_{i,j}$, $i = 1, \cdots, Q$, $j = 1, \cdots, Q$ are elements of the Discrete Fourier Transform (DFT) matrix $\boldsymbol{F}_Q$ of size $Q \times Q$. $\boldsymbol{1}$ denotes all one column vector. $\otimes$ denotes Kronecker product.

The main advantage of the matrix factorized weighted construction of ZCZ sequence is that a fast correlator can be designed which only needs phase rotation operations. Figure 6 illustrates an example of a fast correlator for the ZCZ sequence generated by the method developed by CMMG WLAN standard task group, where the length of the ZCZ sequence, the number of the ZCZ sequences, and the length of the zero correlation zone are 8, 2, and 2, respectively. In Fig. 6, $\boldsymbol{R} = [r_1, \cdots, r_8]$ is a receiving sequence that is correlated with each ZCZ sequence in the set of the ZCZ sequences. $w_{i,j}, i, j = 1, 2$ denote the weight coefficients. $C_{R,Z_i}, i = 1, 2$ denotes the correlation coefficient between the receiving sequence $\boldsymbol{R}$ and the ZCZ sequence $Z_i, i = 1, 2$. α_i and β_i is the initial sequence, $i = 1, 2$. "*" denotes the conjugate operation.

5. LDPC-Based Packet Encoding for CMMG WLAN Standard

Low density parity check code (LDPC) was shown to achieve reliable transmission at a signal-to-noise ratio (SNR) extremely close to the Shannon limit for memoryless binary-input unfaded Gaussian channels [44]. LDPC code is a kind of block Forward Error Correction (FEC) code. According to the knowledge of information theory on coding, it is easy to see that the better coding performance can be achieved with a longer code length of FEC. In practical communication systems, the transmission data packet is divided

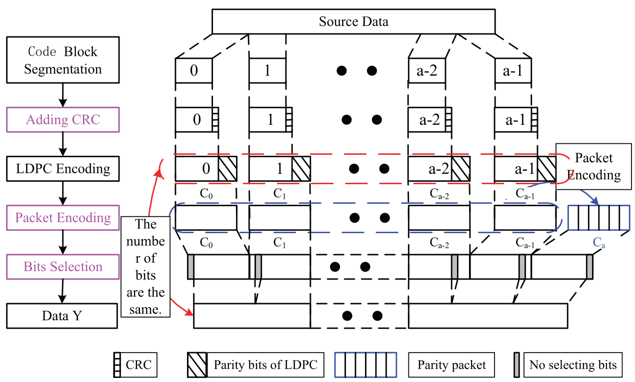

Fig. 7 Flowchart of the LDPC-based packet encoding scheme [39].

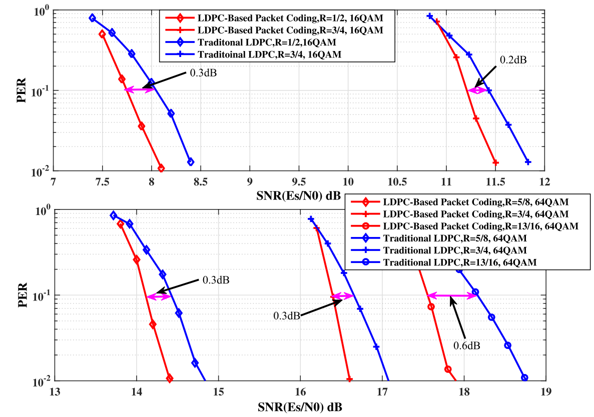

Fig. 8 Flowchart of the LDPC-based coding scheme [39].

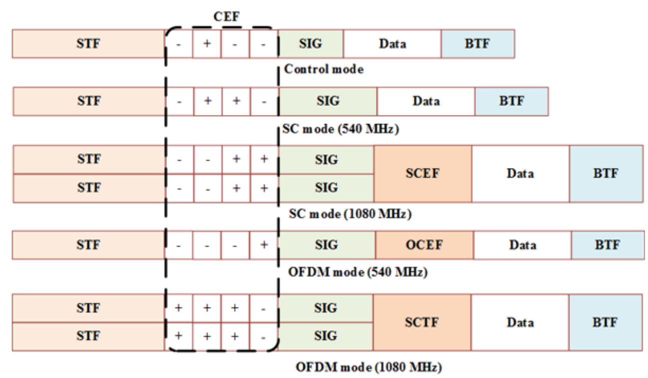

Fig. 9 Format of physical protocol data unit for CMMG WLAN standard.

into some sub-blocks where each sub-block is encoded separately with incurring a certain coding performance loss. It also means that achieving the best coding performance needs to make the coding length as large as possible. As a result, the coding complexity also increases with the coding length.

To further improve the FEC performance and speed up the decoding of the LDPC code, CMMG task group designed a novel LDPC-based packet encoding scheme for CMMG WLAN standard [33]. Figure 7 shows the flowchart of the LDPC-based packet encoding scheme. The details of the LDPC-based packet encoding scheme are described in CMMG WLAN standard [33]. It is easy to see that different from the traditional LDPC encoder, a new cyclic redundancy check subblock is appended for each block of coding information bits. A new packet encoding codeword is generated with bit-wise addition module 2 for all encoded codewords. Furthermore, a puncture operation is adopted via the bit selection operation to avoid introducing additional bits with the packet encoding codeword.

Figure 8 illustrates the performance comparison between the LDPC-based packet encoding scheme and the traditional LDPC encoding scheme [32] for additive Gaussian white noise (AWGN) channel where R denotes the code rate. Simulation results show that compared to the traditional LDPC coding scheme, the LDPC-based packet encoding scheme obtains 0.2 ~ 0.6 dB performance gain in terms of the packet error rate (PER) criterion. The cost of obtaining the improvement of the PER performance is the increasing of two additional operations, i.e., the cyclic redundancy check (CRC) and the bits selection modules. Fortunately, these modules are easily implemented via existing technologies with very lower cost.

6. Transmission Mode of CMMG WLAN Standard

CMMG WLAN standard defined three kinds of transmit modes, i.e., the robust Control mode used to guarantee the coverage, the SC mode, and the OFDM mode, to satisfy various requirements in different environments. The latter two modes have the ability to support diversity and multiplexing transmission via MIMO transmission mechanism.

Figure 9 shows the format of physical protocol data unit (PPDU) for CMMG WLAN standard where "+" and "-" denote respectively the positive sign and minus sign. The CMMG physical (PHY) preamble including the short training field (STF) and the channel estimation field (CEF) is a part of the PHY PPDU and is used for packet detection, automatic gain control (AGC), frequency offset estimation, synchronization, indication of transmission mode (Control mode, SC mode, or OFDM mode), indication of transmission bandwidth (540 MHz or 1080 MHz), and channel estimation. The format of the preamble is common to both SC packets and OFDM packets and consists of a STF followed by a CEF. The content of the STF is the same between SC and OFDM packets, but the content of the CEF is not the same between such packets. In Fig. 9, the pattern of the CEF is used to determine the channel bandwidth, the carrier modulation and the transmission mode [52]. The beam training field (BTF) is used to track the transmitting beam and refine the transmitting or receiving beam. Note that when the channel width is 1080 MHz for SC mode, to effectively estimate the channel state information, an additional SC channel estimation field (SCEF) is inserted between the signaling (SIG) field and the data field. Otherwise, one cannot obtain the channel coefficient for the 1080 MHz channel for SC mode transmission.

Table 2 The Barker sequences.

Length	Barker Sequence
4	+1, +1, -1, +1
7	+1, +1, +1, -1, -1,+1, -1
13	+1, +1, +1, +1, +1, -1, -1, +1, +1, -1, +1, -1, +1

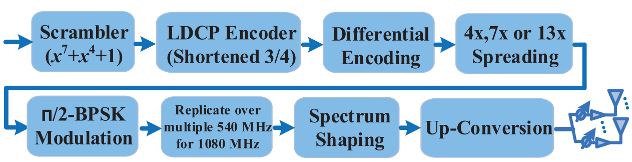

Fig. 10 Transmitter block diagram for control mode.

6.1 Control Mode

The role of the Control mode is to transmit the control information which is used to guarantee the synchronization between the access point (AP) and the user terminal (stations) and the coverage radius of the basic service set. In Control mode, to enhance the robustness of the transmitted signal, the most robust modulation and coding scheme (MCS0), i.e., binary phase shift keying (BPSK) modulation with lowest coding rate, is adopted. Support for MCS0 is mandatory.

The robustness of the control physical layer is evidently from its use of differential encoding, Barker sequence based code spreading and BPSK. The Barker sequence which is used in CMMG WLAN standard is listed in Table 2 [51]. Different from IEEE 802.11ad [32], CMMG WLAN standard supports link adaptation code spreading according to the change of the environments [33].

Figure 10 illustrates the transmission block diagram of the encoding and modulation steps for Control mode where $x^7 + x^4 + 1$ denotes the generation polynomial of the scrambler and 4x, 7x, and 13x denotes respectively the 4, 7, and 13 times spread spectrum operation. In CMMG WLAN standard, the control message transmitted on the 540 MHZ bandwidth with beamforming style is mandatory. If the channel bandwidth is 1080 MHz, the modulated control mode SIG and data field symbols are transmitted with duplicated style to ensure that all stations can receive control message.

6.2 SC Mode

To achieve low peak-to-average power ratio (PAPR) of transmit signal and high transmit data rate, SC mode was introduced for CMMG WLAN standard [33]. Simultaneously, in order to obtain the multiplexing gains, CMMG WLAN standard also supports SC multi-streams transmission mechanism with using a unique words (UW) as guard interval (GI) to avoid the inter-symbol interference (ISI) occurred by the multiple paths. Furthermore, the length of the UW is larger than that of the channel taps for removing inter-block interference. Figure 11 shows the transmission block diagram for the SIG field of SC mode. When the transmitter is equipped with multiple transmit antennas, the classical cyclic shift diversity technology is used to extending the SIG field to the multiple transmit antennas.

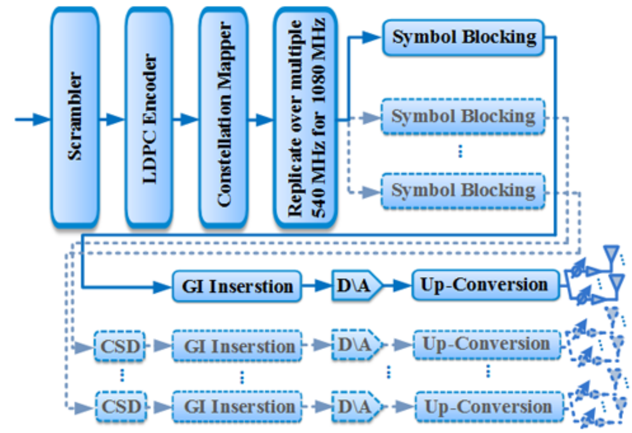

Fig. 11 Transmitter block diagram for the SIG field of SC mode.

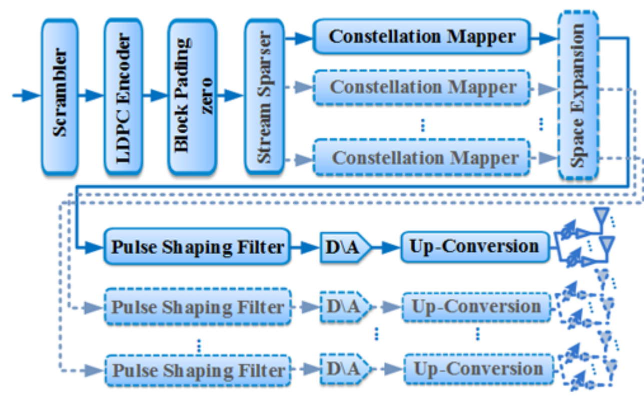

Fig. 12 Transmitter block diagram for data fields of SC mode PPDUs.

As shown in Fig. 12, the SC format transmission adopted UW-based space time blocking code for supporting MIMO operation can be generated using a transmitter consisting of the following blocks:

- Scrambler: The scrambling of the Data field continues the scrambling of the SC mode SIG with no reset for SC mode transmission.
- LDPC encoding: The scrambled bits are encoded by using LDPC-based packet encoding scheme introduced in Sect. 5.
- Block padding zero: To guarantee the number of coded bits is the integer times of the N_{CBPB}, where N_{CBPB} is the number of coded bits included in each block and is defined in Table 3.
- Stream parser: Rearrange the output of the LDPC encoders and block padding zeros into blocks.
- Constellation mapper: Mapping the bit sequence in each spatial stream to $\pi/2$-BPSK, $\pi/2$-QPSK, $\pi/2$-16QAM, or $\pi/2$-64QAM constellation.
- Spatial expansion: Spreading constellation points from

IEICE TRANS. COMMUN., VOL.E101–B, NO.2 FEBRUARY 2018

Index	N_{SS}	N_{TXT}	i_{TXT}	$\tilde{\mathbf{x}}_{i_{TXT}, 2^a m}$	$\tilde{\mathbf{x}}_{i_{TXT}, 2^a m+1}$	$\tilde{\mathbf{x}}_{i_{TXT}, 2^a m+2}$	$\tilde{\mathbf{x}}_{i_{TXT}, 2^a m+3}$
1	1	1	1	$\tilde{\mathbf{d}}_{1, 2^a m} + \tilde{\mathbf{u}}_{i_{TXT}}$	$\tilde{\mathbf{d}}_{1, 2^a m+1} + \tilde{\mathbf{u}}_{i_{TXT}}$	-	-
2		2	1	$\tilde{\mathbf{d}}_{1, 2^a m} + \tilde{\mathbf{u}}_{i_{TXT}}$	$-\mathbf{Q}_{N_{BLS}}\tilde{\mathbf{d}}^*_{1, 2^a m+1} + \tilde{\mathbf{u}}_{i_{TXT}}$	-	-
			2	$\tilde{\mathbf{d}}_{1, 2^a m+1} + \tilde{\mathbf{u}}_{i_{TXT}}$	$\mathbf{Q}_{N_{BLS}}\tilde{\mathbf{d}}^*_{1, 2^a m} + \tilde{\mathbf{u}}_{i_{TXT}}$	-	-
3		3	1	$\tilde{\mathbf{d}}_{1, 3m} + \tilde{\mathbf{u}}_{i_{TXT}}$	$\mathbf{Q}_{N_{BLS}}\tilde{\mathbf{d}}^*_{1, 3m+1} + \tilde{\mathbf{u}}_{i_{TXT}}$	$\mathbf{Q}_{N_{BLS}}\tilde{\mathbf{d}}^*_{1, 3m+2} + \tilde{\mathbf{u}}_{i_{TXT}}$	$\mathbf{0}$
			2	$-\tilde{\mathbf{d}}_{1, 3m+1} + \tilde{\mathbf{u}}_{i_{TXT}}$	$\mathbf{Q}_{N_{BLS}}\tilde{\mathbf{d}}^*_{1, 3m} + \tilde{\mathbf{u}}_{i_{TXT}}$	$\mathbf{0}$	$-\mathbf{Q}_{N_{BLS}}\tilde{\mathbf{d}}^*_{1, 3m+2} + \tilde{\mathbf{u}}_{i_{TXT}}$
			3	$-\tilde{\mathbf{d}}_{1, 3m+2} + \tilde{\mathbf{u}}_{i_{TXT}}$	$\mathbf{0}$	$\mathbf{Q}_{N_{BLS}}\tilde{\mathbf{d}}^*_{1, 3m} + \tilde{\mathbf{u}}_{i_{TXT}}$	$\mathbf{Q}_{N_{BLS}}\tilde{\mathbf{d}}^*_{1, 3m+1} + \tilde{\mathbf{u}}_{i_{TXT}}$
4		4	1	$\tilde{\mathbf{d}}_{1, 2^a m} + \tilde{\mathbf{u}}_{i_{TXT}}$	$-\mathbf{Q}_{N_{BLS}}\tilde{\mathbf{d}}^*_{1, 2^a m+1} + \tilde{\mathbf{u}}_{i_{TXT}}$	$-\mathbf{Q}_{N_{BLS}}\tilde{\mathbf{d}}^*_{1, 2^a m+2} + \tilde{\mathbf{u}}_{i_{TXT}}$	$\tilde{\mathbf{d}}_{1, 2^a m+3} + \tilde{\mathbf{u}}_{i_{TXT}}$
			2	$\tilde{\mathbf{d}}_{1, 2^a m+1} + \tilde{\mathbf{u}}_{i_{TXT}}$	$\mathbf{Q}_{N_{BLS}}\tilde{\mathbf{d}}^*_{1, 2^a m} + \tilde{\mathbf{u}}_{i_{TXT}}$	$-\mathbf{Q}_{N_{BLS}}\tilde{\mathbf{d}}^*_{1, 2^a m+3} + \tilde{\mathbf{u}}_{i_{TXT}}$	$-\tilde{\mathbf{d}}_{1, 2^a m+2} + \tilde{\mathbf{u}}_{i_{TXT}}$
			3	$\tilde{\mathbf{d}}_{1, 2^a m+2} + \tilde{\mathbf{u}}_{i_{TXT}}$	$-\mathbf{Q}_{N_{BLS}}\tilde{\mathbf{d}}^*_{1, 2^a m+3} + \tilde{\mathbf{u}}_{i_{TXT}}$	$\mathbf{Q}_{N_{BLS}}\tilde{\mathbf{d}}^*_{1, 2^a m} + \tilde{\mathbf{u}}_{i_{TXT}}$	$-\tilde{\mathbf{d}}_{1, 2^a m+1} + \tilde{\mathbf{u}}_{i_{TXT}}$
			4	$\tilde{\mathbf{d}}_{1, 2^a m+3} + \tilde{\mathbf{u}}_{i_{TXT}}$	$\mathbf{Q}_{N_{BLS}}\tilde{\mathbf{d}}^*_{1, 2^a m+2} + \tilde{\mathbf{u}}_{i_{TXT}}$	$\mathbf{Q}_{N_{BLS}}\tilde{\mathbf{d}}^*_{1, 2^a m+1} + \tilde{\mathbf{u}}_{i_{TXT}}$	$\tilde{\mathbf{d}}_{1, 2^a m} + \tilde{\mathbf{u}}_{i_{TXT}}$
5	2	2	1	$\tilde{\mathbf{d}}_{1, 2^a m} + \tilde{\mathbf{u}}_{i_{TXT}}$	$\tilde{\mathbf{d}}_{1, 2^a m+1} + \tilde{\mathbf{u}}_{i_{TXT}}$	-	-
			2	$\tilde{\mathbf{d}}_{2, 2^a m} + \tilde{\mathbf{u}}_{i_{TXT}}$	$\tilde{\mathbf{d}}_{2, 2^a m+1} + \tilde{\mathbf{u}}_{i_{TXT}}$	-	-
6		3	1	$\tilde{\mathbf{d}}_{1, 2^a m} + \tilde{\mathbf{u}}_{i_{TXT}}$	$-\mathbf{Q}_{N_{BLS}}\tilde{\mathbf{d}}^*_{1, 2^a m+1} + \tilde{\mathbf{u}}_{i_{TXT}}$	-	-
			2	$\tilde{\mathbf{d}}_{1, 2^a m+1} + \tilde{\mathbf{u}}_{i_{TXT}}$	$\mathbf{Q}_{N_{BLS}}\tilde{\mathbf{d}}^*_{1, 2^a m} + \tilde{\mathbf{u}}_{i_{TXT}}$	-	-
			3	$\tilde{\mathbf{d}}_{2, 2^a m} + \tilde{\mathbf{u}}_{i_{TXT}}$	$\mathbf{Q}_{N_{BLS}}\tilde{\mathbf{d}}^*_{2, 2^a m+1} + \tilde{\mathbf{u}}_{i_{TXT}}$	-	-
7		4	1	$\tilde{\mathbf{d}}_{1, 2^a m} + \tilde{\mathbf{u}}_{i_{TXT}}$	$-\mathbf{Q}_{N_{BLS}}\tilde{\mathbf{d}}^*_{1, 2^a m+1} + \tilde{\mathbf{u}}_{i_{TXT}}$	-	-
			2	$\tilde{\mathbf{d}}_{1, 2^a m+1} + \tilde{\mathbf{u}}_{i_{TXT}}$	$\mathbf{Q}_{N_{BLS}}\tilde{\mathbf{d}}^*_{1, 2^a m} + \tilde{\mathbf{u}}_{i_{TXT}}$	-	-
			3	$\tilde{\mathbf{d}}_{2, 2^a m} + \tilde{\mathbf{u}}_{i_{TXT}}$	$-\mathbf{Q}_{N_{BLS}}\tilde{\mathbf{d}}^*_{2, 2^a m+1} + \tilde{\mathbf{u}}_{i_{TXT}}$	-	-
			4	$\tilde{\mathbf{d}}_{2, 2^a m+1} + \tilde{\mathbf{u}}_{i_{TXT}}$	$\mathbf{Q}_{N_{BLS}}\tilde{\mathbf{d}}^*_{2, 2^a m} + \tilde{\mathbf{u}}_{i_{TXT}}$	-	-
8	3	3	1	$\tilde{\mathbf{d}}_{1, 2^a m} + \tilde{\mathbf{u}}_{i_{TXT}}$	$\tilde{\mathbf{d}}_{1, 2^a m+1} + \tilde{\mathbf{u}}_{i_{TXT}}$	-	-
			2	$\tilde{\mathbf{d}}_{2, 2^a m} + \tilde{\mathbf{u}}_{i_{TXT}}$	$\tilde{\mathbf{d}}_{2, 2^a m+1} + \tilde{\mathbf{u}}_{i_{TXT}}$	-	-
			3	$\tilde{\mathbf{d}}_{3, 2^a m} + \tilde{\mathbf{u}}_{i_{TXT}}$	$\mathbf{d}_{3, 2^a m+1} + \tilde{\mathbf{u}}_{i_{TXT}}$	-	-
9		4	1	$\tilde{\mathbf{d}}_{1, 2^a m} + \tilde{\mathbf{u}}_{i_{TXT}}$	$-\mathbf{Q}_{N_{BLS}}\tilde{\mathbf{d}}^*_{1, 2^a m+1} + \tilde{\mathbf{u}}_{i_{TXT}}$	-	-
			2	$\tilde{\mathbf{d}}_{1, 2^a m+1} + \tilde{\mathbf{u}}_{i_{TXT}}$	$\mathbf{Q}_{N_{BLS}}\tilde{\mathbf{d}}^*_{1, 2^a m} + \tilde{\mathbf{u}}_{i_{TXT}}$	-	-
			3	$\tilde{\mathbf{d}}_{2, 2^a m} + \tilde{\mathbf{u}}_{i_{TXT}}$	$\mathbf{Q}_{N_{BLS}}\tilde{\mathbf{d}}_{2, 2^a m+1} + \tilde{\mathbf{u}}_{i_{TXT}}$	-	-
			4	$\tilde{\mathbf{d}}_{3, 2^a m} + \tilde{\mathbf{u}}_{i_{TXT}}$	$\mathbf{Q}_{N_{BLS}}\tilde{\mathbf{d}}_{3, 2^a m+1} + \tilde{\mathbf{u}}_{i_{TXT}}$	-	-
10	4	4	1	$\tilde{\mathbf{d}}_{1, 2^a m} + \tilde{\mathbf{u}}_{i_{TXT}}$	$\tilde{\mathbf{d}}_{1, 2^a m+1} + \tilde{\mathbf{u}}_{i_{TXT}}$	-	-
			2	$\tilde{\mathbf{d}}_{2, 2^a m} + \tilde{\mathbf{u}}_{i_{TXT}}$	$\tilde{\mathbf{d}}_{2, 2^a m+1} + \tilde{\mathbf{u}}_{i_{TXT}}$	-	-
			3	$\tilde{\mathbf{d}}_{3, 2^a m} + \tilde{\mathbf{u}}_{i_{TXT}}$	$\tilde{\mathbf{d}}_{3, 2^a m+1} + \tilde{\mathbf{u}}_{i_{TXT}}$	-	-
			4	$\tilde{\mathbf{d}}_{4, 2^a m} + \tilde{\mathbf{u}}_{i_{TXT}}$	$\tilde{\mathbf{d}}_{4, 2^a m+1} + \tilde{\mathbf{u}}_{i_{TXT}}$	-	-

NOTE 1—a=2, for $N_{SS} = 1$ and $N_{TXT} = 4$, otherwise a=1.
NOTE 2— * indicates conjugate operation.

Fig. 13 Spatial expansion mechanism of SC mode.

Table 3 Values of N_{CBPB}.

Mapper	540 MHz		1080 MHz	
	Long GI	Short GI	Long GI	Short GI
$\pi/2$-BPSK	192	224	384	448
$\pi/2$-QPSK	384	448	768	896
$\pi/2$-16QAM	768	896	1536	1792
$\pi/2$-64QAM	1152	1344	2304	2688

N_{ss} spatial streams into N_{STS} space time streams using a specific spatial expansion mechanism.

- Pulse shaping filter: Filtering the signal to shape transmit signal spectrum.
- Analog and RF: Up-converting the resulting complex baseband waveform associated with each transmit chain to an RF signal according to the center frequency of the desired channel and transmit.

In practical communication implementation, the number of the spatial streams may different from that of the transmitting antennas. Thus, the question arises of how to map fewer spatial streams to more transmit antenna chains without causing unintentional beamforming and making the best use of the available power amplifiers and transmit chains. To reduce the feedback overhead, an open loop spatial expansion mechanism, i.e., UW-based space time block coding spatial expansion, is proposed for SC mode with MIMO transmission. Note that the UW in every block is the same for mth transmit antenna, thus fulfilling the theorem of circular convolution. To reduce the correlation between the streams transmitted by different transmitting antennas, a conjunction operation and a permutation operation are introduced in the spatial expansion mechanism. Figure 13 defines the spatial expansion mechanism of different spatial stream for SC mode with MIMO transmission systems.

In Fig. 13, $\widetilde{\boldsymbol{d}}_{i,j}$ denotes jth data block of the ith spatial stream. $\widetilde{\boldsymbol{x}}_{i,j}$ denotes the jth data block of the ith transmit antenna. $\widetilde{\boldsymbol{u}}_i$ denotes the UW transmitted at the ith transmit antenna. $\boldsymbol{Q}_{\mathrm{N_{BLS}}}$ is an $N_{BLS} \times N_{BLS}$ spatial expansion matrix, where N_{BLS} is the number of symbols in each transmit block for SC mode, and is given by

$$\boldsymbol{Q}_{\mathrm{N_{BLS}}} = \begin{pmatrix} \boldsymbol{Q}_1 & \boldsymbol{Q}_2 \\ \boldsymbol{Q}_3 & \boldsymbol{Q}_4 \end{pmatrix}$$

where $\boldsymbol{Q}_2 = \mathbf{0}_{\mathrm{N_{DSPB}} \times \mathrm{N_{UWPB}}}$, $\boldsymbol{Q}_3 = \mathbf{0}_{\mathrm{N_{UWPB}} \times \mathrm{N_{DSPB}}}$, and

$$\boldsymbol{Q}_3 = \begin{pmatrix} 0 & 0 & 0 & \cdots & 0 & 0 & 1 \\ 0 & 0 & 0 & \cdots & 0 & 1 & 0 \\ \vdots & \vdots & \vdots & \ddots & \vdots & \vdots & \vdots \\ 0 & 1 & 0 & \cdots & 0 & 0 & 0 \\ 1 & 0 & 0 & \cdots & 0 & 0 & 0 \end{pmatrix}_{\mathrm{N_{DSPB}} \times \mathrm{N_{DSPB}}}$$

$$\boldsymbol{Q}_3 = \begin{pmatrix} 0 & 0 & 0 & \cdots & 0 & 0 & 1 \\ 0 & 0 & 0 & \cdots & 0 & 1 & 0 \\ \vdots & \vdots & \vdots & \ddots & \vdots & \vdots & \vdots \\ 0 & 1 & 0 & \cdots & 0 & 0 & 0 \\ 1 & 0 & 0 & \cdots & 0 & 0 & 0 \end{pmatrix}_{\mathrm{N_{UWPB}} \times \mathrm{N_{UWPB}}}$$

The values of N_{DSPB} and N_{UWPB} are given in Table 4. The

Table 4 Values of N_{DSPB} and N_{UWPB}

	540 MHz		1080 MHz	
	Long GI	Short GI	Long GI	Short GI
N_{DSPB}	192	224	384	448
N_{UWPB}	64	32	128	64

Fig. 14 Block transmission structure of SC mode PPDUs.

Fig. 15 Physical protocol data unit format of OFDM mode.

Table 5 Comparison of PAPR

	PAPR	
	Length of 256	Length of 512
11ac LTF	8.6 dB	11.6 dB
CMMG OCEF	3.2 dB	3.6 dB

UW is composed of the ZCZ sequence of length 32, 62, or 128 generated by the matrix factorized weighted construction method introduced in Sect. 4.

Figure 14 illustrates the structure of the physical protocol data unit of SC mode. After the transmission block generation is finished, an additional UW which is the same with that of the data block needs to be prepended to the first block transmitted.

In summary, the SC mode in CMMG WLAN standard can obtain simultaneously the transmission diversity and multiplex gains via the spatial multiplexing mechanism and the array antennas technology.

6.3 OFDM Mode

OFDM mode is an optional transmission mechanism for CMMG WLAN standard. With regard to the choice of SC mode or OFDM mode, the generally accepted reason for favouring one over the other is the relative importance, in a given application, of power consumption (i.e., maximizing battery life) compared with maximizing data throughput.

Similarly, OFDM mode simultaneously supports diversity transmission and diversity-multiplexing transmission. Different from SC mode, in OFDM mode, the spatial expansion mechanism can be designed based on the feedback of the channel state information subject to certain performance criterion. Figure 15 illustrates the PPDU format of the OFDM mode for CMMG WLAN standard. An obvious difference between SC mode and OFDM mode is that CMMG WLAN task group designed a new short training field (OSTF) and channel estimation field (OCEF) to adapt the estimation of an effective channel state information. The specific definition of the OSTF sequence and the OCEF sequence are given in Sect. 8. The comparison of PAPR between the OCEF in CMMG WLAN standard and the long train field in IEEE 802.11ac is listed in Table 5.

7. Performance Evaluation

In this section, the performance of the CMMG WLAN system is evaluated via numerical results and the test of the prototype. Table 6 lists the modulation and coding schemes used in the CMMG WLAN standard, includes the BPSK, quadrature phase shift keying (QPSK), and quadrature amplitude modulation (QAM). In our simulation, the CMMG channel is generated according to the methods described in [53], [54].

Table 6 Modulation and coding schemes (MCS) for CMMG WLAN standard.

MCS Index	0	1	2	3	4	5	6	7
Modulation	BPSK	QPSK		16QAM		64QAM		
Code Rate	1/2	1/2	3/4	1/2	3/4	5/8	3/4	15/16

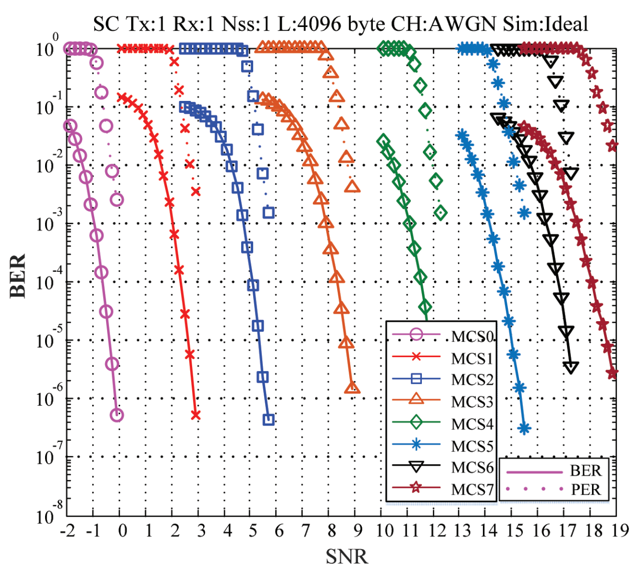

Fig. 16 Performance comparison of SC mode for the additive Gaussian white noise (AWGN) channel.

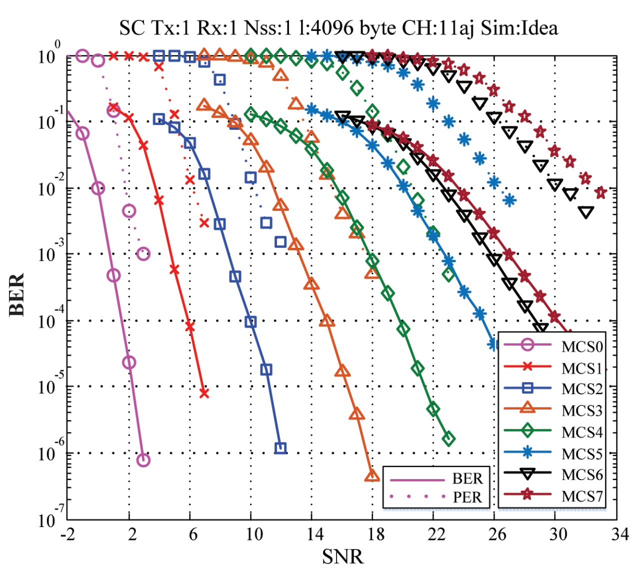

Fig. 17 Performance comparison of SC mode for the CMMG channel.

7.1 Numerical Results

Figure 16 and Fig. 17 illustrate the performance comparison of SC mode between the additive Gaussian white noise (AWGN) channel and CMMG WLAN fading channel without taking any hardware impairment into account for single input single output system. Numerical results show that the performance in CMMG WLAN fading channel is much lower than that in AWGN channel due to the impact of the fading characteristic of the millimeter wave propagation channel. When PER= 10^{-1}, the performance deterioration

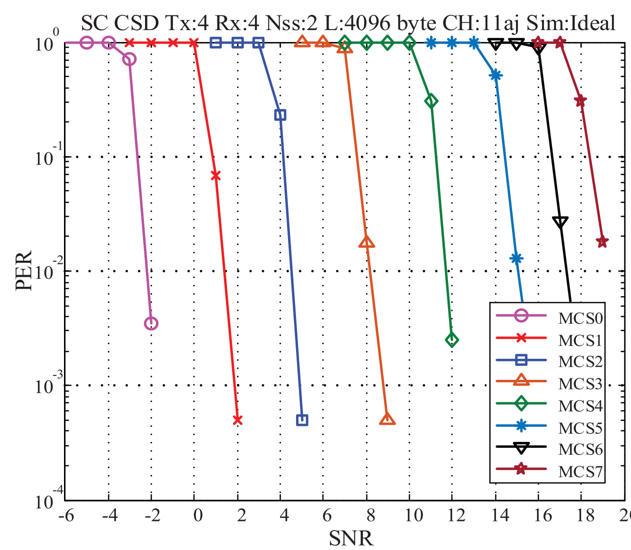

Fig. 18 Performance comparison of SC mode for the CMMG channel with cycle shift diversity spatial expansion mechanism.

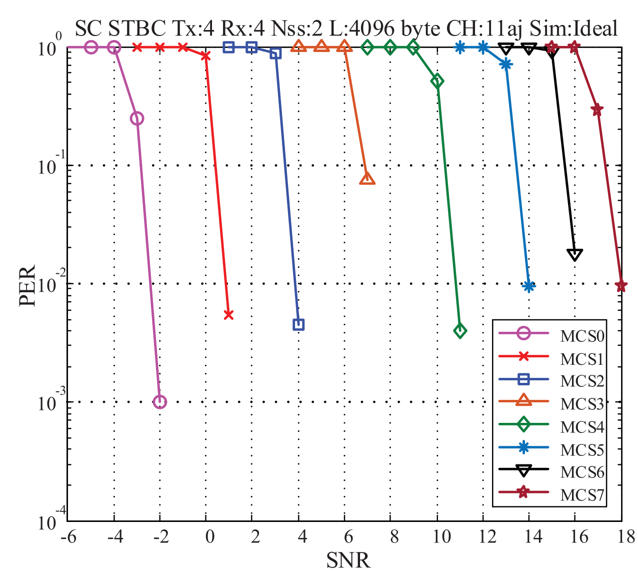

Fig. 19 Performance comparison of SC mode for the CMMG channel with space time block coding spatial expansion mechanism.

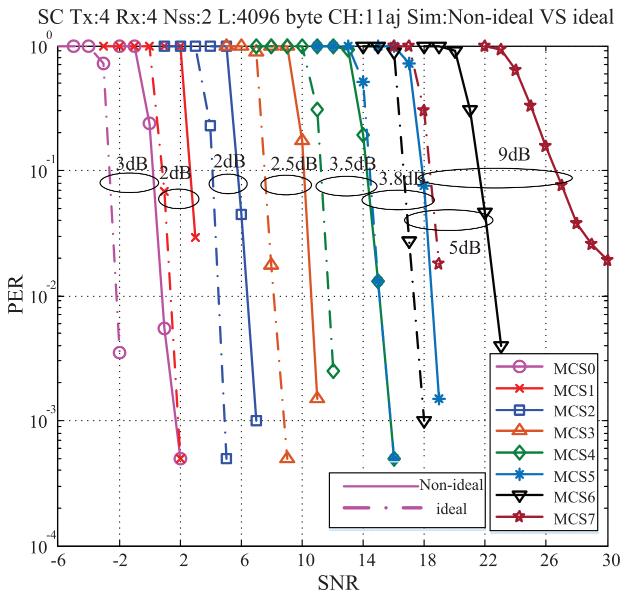

Fig. 20 Performance comparison of SC mode for the CMMG channel with space time block coding spatial expansion mechanism IQ: 1 dB, 2^o, PA backoff: 3 dB, Carrier frequency offset: 615 kHz.

of high-order MCS is about 10 dB, so we need to consider using multiple antennas technology to compensate the path loss incurred by the mmWave propagation channel.

Figure 18 and Fig. 19 illustrate the performance comparison of the two spatial streams transmitted by SC mode with different spatial expansion mechanism. Numerical results show that the space time block coding spatial expansion mechanism outperforms the cyclic shift diversity spatial expansion mechanism in terms of the packet error rate with a steeper slope.

Figure 20 illustrates the performance of SC mode for the CMMG WLAN fading channel with space time block coding spatial expansion mechanism with taking the impaction of the hardware impairment account. Numerical results illustrate that when the impaction of the hardware impairment, such as I/Q imbalance, power amplifier backoff, phase noise, etc, cannot be ignored, the performance of SC mode become worse with 2 – 9 dB. It also implies that in practice, we need to design hardware impairment compensation algorithm to reduce the impaction of the hardware impairment on the performance of the communication systems.

7.2 System Prototype

In this subsection, we briefly describe the prototype test platform for CMMG WLAN standard. Figure 21 shows the prototype test platform and the related parameters of the system prototype. The transmitter is equipped with 2 transmitting antennas and the receiver is equipped with 4 receiving antennas.

To evaluate the practical performance of the wireless transmission of the developed scheme for the CMMG WLAN standard, a field test is carried in two scenarios, i.e., the laboratory and the corridor in a building, illustrated in Fig. 22. The performance of the field test of the prototype is shown in Fig. 23. Field test results show that the designed scheme for the CMMG WLAN standard can achieves 4.085 Gbps data rate by transmitting two spatial streams with $\frac{3}{4}$ code rate, 64 QAM modulation, and 540 MHz transmission bandwidth. Field test results also validate that the mmWave frequency bands have the ability to achieve spatial multiplexing transmission and to achieve small cell hot-spot coverage.

Parameters	Values
Carrier Frequency	42.795 GHz
Middle Frequency	5.77 GHz
Bandwidth	500MHz
Number of Transmit antennas	2
Number of Transmit antennas	4
Peak Rate	4095Mbps
Number of spatial streams	2
MCS	SC , ¾ LDPC , 64QAM
Distance between transmitter and receiver	5~14, 20~85;
Environment	Indoor

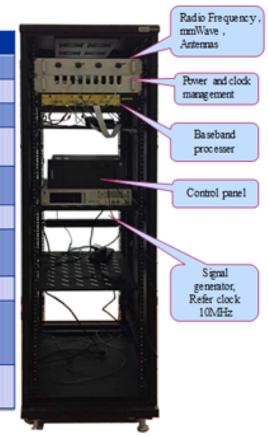

Fig. 21 Prototype machine of CMMG WLAN standard.

Fig. 22 Test environment of CMMG WLAN standard.

Fig. 23 Test performance of CMMG WLAN standard.

8. Conclusion

This paper provided an overview of the key technologies adopted in the CMMG WLAN standard and the progress of CMMG WLAN standardization. CMMG WLAN standard supports three transmission modes, i.e., Control mode, SC mode, and OFDM mode. The first two transmission modes are mandatory and the third transmission mode is optional. The zero correlation zone sequence was adopted as the training sequence. To enhance the robustness of the transmitted data, a novel LDPC-based packet encoding scheme was developed for CMMG WLAN standard. Extensive numerical results and field test results of a system prototype are provided to verify the effectiveness of the key technologies developed for the CMMG WLAN standard.

References

[1] Cisco, "Cisco visual network index: Global mobile traffic forecast update," 2013.
[2] Ericsson, "Traffic and market data report," 2011.
[3] UMTS Forum, "Mobile traffic forecasts: 20102020 report," vol.44, 2011.
[4] Z. Pi and F. Khan, "An introduction to millimeter-wave mobile broadband systems," IEEE Commun. Mag., vol.49, no.6, pp.101–07, June 2011.
[5] T. Rappaport, J. Nurdock, and F. Gutierrez, "State of the art in 60-GHz integrated circuits and systems for wireless communications," Proc. IEEE, vol.99, no.8, pp.1390–1436, Aug. 2011.
[6] F. Khan and Z. Pi, "Millimeter wave mobile broadband (MMB): Unleashing the 3–C300 GHz spectrum," Proc. 34th IEEE Sarnoff Symp., March 2011, DOI: 10.1109/SARNOF.2011.5876482.
[7] P. Pietraski, D. Britz, A. Roy, R. Pragada, and G. Charlton, "Millimeter wave and terahertz communications: Feasibility and challenges," ZTE Commun., vol.10, no.4, pp.3–C12, Dec. 2012.
[8] S. Hur, T. Kim, D. Love, J. Krogmeier, T. Thomas, and A. Ghosh, "Millimeter wave beamforming for wireless backhaul and access in small cell networks," IEEE Trans. Commun., vol.61, no.10, pp.4391–4403, Oct. 2013.
[9] V. Venkateswaran and A. van der Veen, "Analog beamforming in MIMO communications with phase shift networks and online channel estimation," IEEE Trans. Sig. Proc., vol.58, no.8, pp.4131–4143, Aug. 2010.
[10] X. Zhang, A. Molisch, and S. Kung, "Variable-phase-shift-based RF-baseband codesign for MIMO antenna selection," IEEE Trans. Signal Process., vol.53, no.11, pp.4091–4103, Nov. 2005.
[11] T. Rappaport, S. Sun, R. Mayzus, H. Zhao, Y. Azar, K. Wang, G.N. Wong, J.K. Schulz, M. Samimi, and F. Gutierrez, "Millimeter wave mobile communications for 5G cellular: It will work!," IEEE Access, vol.1, pp.335–349, 2013.
[12] C. Doan, S. Emami, D. Sobel, A. Niknejad, and R. Brodersen, "Design considerations for 60 GHz CMOS radios," IEEE Commun. Mag., vol.42, no.12, pp.132–140, Dec. 2004.
[13] C. Doan, S. Emami, A. Niknejad, and R. Brodersen, "Millimeter wave CMOS design," IEEE J. Solid-State Circuits, vol.40, no.1, pp.144–155, Jan. 2005.
[14] Y. Zhang and D. Liu, "Antenna-on-chip and antenna-in-package solutions to highly integrated millimeter wave devices for wireless communications," IEEE Trans. Antennas Propag., vol.57, no.10, pp.2830–2841, Oct. 2009.
[15] F. Gutierrez, S. Agarwal, K. Parrish, and T.S. Rappaport, "On-chip integrated antenna structures in CMOS for 60 GHz WPAN systems," IEEE J. Sel. Areas Commun., vol.27, no.8, pp.1367–1378, Oct. 2009.
[16] J. Nsenga, A. Bourdoux, and F. Horlin, "Mixed analog/digital beamforming for 60 GHz MIMO frequency selective channels," Proc. IEEE Int. Conf. Commun., 2010, DOI: 10.1109/ICC.2010.5502689.
[17] J. Wang, Z. Lan, C.-W. Pyo, T. Baykas, C.-S. Sum, M.A. Rahman, J. Gao, R. Funada, F. Kojima, H. Harada, and S. Kato, "Beam codebook based beamforming protocol for multiGbps millimeter-wave WPAN systems," IEEE J. Sel. Areas Commun., vol.27, no.8, pp.1390–1399, Aug. 2009.
[18] T. Rappaport, F. Gutierrez, E. Ben-Dor, J. Murdock, Y. Qiao, and J. Tamir, "Broadband millimeter-wave propagation measurements and models using adaptive-beam antennas for outdoor urban cellular communications," IEEE Trans. Antennas Propag., vol.61, no.4, pp.1850–1859, April 2013.
[19] C. Dehos, J.L. Gonzalez, A. De Domenico, D. Ktenas, and L. Dussopt, "Millimeter-wave access and backhauling: The solution to the exponential data traffic increase in 5G Mobile communications systems?" IEEE Commun. Mag., vol.52, no.9, pp.88–95, Sept. 2014.
[20] S. Rangan, T. Rappaport, and E. Erkip, "Millimeter-wave cellular wireless networks: Potentials and challenges," Proc. IEEE, vol.102, nno.3, pp.366–385, March 2014.
[21] L. Liang, W. Xu, and X. Dong, "Low-complexity hybrid precoding in massive multiuser MIMO systems," IEEE Commun. Lett., vol.3, no.6, pp.653–656, Dec. 2014.
[22] O. El Ayach, S. Rajagopal, S. Abu-Surra, Z. Pi, and R. Heath, "Spatially sparse precoding in millimeter wave MIMO systems," IEEE Trans. Wireless Commun., vol.13, no.3, pp.1499–1513, March 2014.
[23] A. Alkhateeb, O. El Ayach, G. Leus, and R. Heath, "Channel estimation and hybrid precoding for millimeter wave cellular systems," IEEE J. Sel. Topics Signal Process., vol.8, no.5, pp.831–846, Oct. 2014.
[24] A. Alkhateeb, G. Leus, and R. Heath, Jr., "Limited feedback hybrid precoding for multi-user millimeter wave systems," IEEE Trans. Wireless Commun., vol.14, no.11, pp.6481–6494, Nov. 2015.
[25] K. Zheng, L. Zhao, J. Mei, M. Dohler, W. Xiang, and Y. Peng, "10 Gb/s HetSNets with millimeter-wave communications: Access and networking challenges and protocols," IEEE Commun. Mag., vol.53, no.1, pp.222–31, Jan. 2015.
[26] R. Baldemair, T. Irnich, K. Balachandran, E. Dahlman, G. Mildh, Y. Selén, S. Parkvall, M. Meyer, and A. Osseiran, "Ultra-dense networks in millimeter-wave frequencies," IEEE Commun. Mag., vol.53, no.1, pp.202–208, Jan. 2015.
[27] R. Heath Jr., N. Gonzalez-Prelcic, S. Rangan, W. Roh, and A. Sayeed, "An overview of signal processing techniques for millimeter wave MIMO systems," IEEE J. Sel. Topics Signal Process., vol.10, no.4, pp.436–453, April 2016.
[28] S. Kutty, and D. Sen, "Beamforming for millimeter wave communications: An inclusive survey," IEEE Commun. Surveys Tuts., vol.18, no.2, pp.949–973, Second Quarter 2016.
[29] "Part 15.3: Wireless MAC and PHY specifications for high rate WPANs. Amendment 2: Millimeter-wave-based alternative physical layer extension," IEEE Std 802.15.3c-2009, Oct. 2009.
[30] WirelessHD, "Specification version 1.1 overview," May 2010.
[31] ECMA International Standard, ECMA-387 High Rate 60 GHz PHY, MAC and HDMI PALs, 2nd ed., Dec. 2010 [Online]. Available: http://www.ecma-international.org/publications/files/ECMA-ST/ECMA-387.pdf
[32] "Part 11: Wireless LAN medium access control (MAC) and physical layer (PHY) specifications. Amendment 3: Enhancements for very high throughput in the 60 GHz band," IEEE Std. 802.11ad-2012, Dec. 2012.
[33] "Part 11: Wireless LAN medium access control (MAC) and physical layer (PHY) specifications. Amendment 5: Enhancements for very high throughput to support chinese millimeter wave frequency bands (60 GHz and 45 GHz)," IEEE Std. 802.11aj-2016, Dec. 2016.
[34] WGA-D1.0, "Wireless gigabit alliance draft specification," July

2010.

[35] C. Hansen, “WiGiG: Multi-gigabit wireless communications in the 60 GHz band,” IEEE Wireless Commun., vol.18, no.6, pp.6–7, Dec. 2011.

[36] “Part 11: Wireless LAN Medium Access Control (MAC) and Physical Layer (PHY) Specifications,” IEEE Std. 802.11-2016, Dec. 2016.

[37] E. Perahia, IEEE 802 11 CMMW SG PAR in NESCOM FORM, IEEE 802.11-12/948r0, 2012.

[38] S. He, H, Wang, Y. Huang, W. Hong, et al., Complete proposal for IEEE 802.11aj 45 GHz, IEEE 802.11-15/0707r1, 2015.

[39] L. Li, J. Xu, Z. Yuan, B. Sun, K. Yao, K. Tian, S. He, and H. Wang, Packet encoding solution for IEEE 802.11aj (45 GHz), IEEE 802.11-14/1387, 2014.

[40] E. Perahia, IEEE 802 11 CMMW SG 5C’s, IEEE 802.11-12/141r7, 2012.

[41] H. Wang, H. Wei, J. Chen, B. Sun, and X. Peng, “IEEE 802.11aj (45 GHz): A new very high throughput millimeter-wave WLAN systems,” China Commun., vol.11, no.6, pp.51–62, June 2014.

[42] MIIT, The usage of 40-50 GHz frequency band for mobile services in broadband wireless access systems, Oneline: http://www.miit.gov.cn/n11293472/n11293832/n12845605/n13916913/15636214.html

[43] X. Peng, H. Wei, L. Li, and Z. Lan, China wpan mmwave liaison for IEEE 802.aj, IEEE 802.11-11/1034, 2011.

[44] T.J. Richardson, M.A. Shokrollahi, and R.L. Urbanke, “Design of capacity-approaching irregular low-density parity-check codes,” IEEE Trans. Inf. Theory, vol.47, no.2, pp.619–637, Feb. 2001.

[45] Y. Wang, S. He, Y. Sun, Q. Xu, H. Wang, and L. Yang, “Joint timing synchronization and channel estimation based on ZCZ sequence set in SC-MIMO-FDE system,” EURASIP Journal on Wireless Communications and Networking, vol.2016, no.1, pp.1–17, 2016.

[46] H. Wang, X. Gao, B. Jiang, X. You, and W. Hong, “Efficient MIMO channel estimation using complementary sequences,” IET Commun., vol.1, no.5, pp.962–969, Oct. 2007.

[47] H. Wang, W. Hong, et al., Channel measurement for IEEE 802.11aj (45 GHz). IEEE 802.11-12/1361r3, 2013.

[48] J. Chen, X. Peng, et al., IEEE 802.11aj usage models document, IEEE 802.11-12/1245r4, 2013.

[49] J. Zhu, H. Wang, and W. Hong, “Large-scale fading characteristics of indoor channel at 45-GHz band,” IEEE Antennas Wireless Propag. Lett., vol.14, pp.735–738, 2015.

[50] P. Fan, “Spreading sequence design and theoretical limits for quasisynchronous CDMA systems,” EURASIP Journal on Wireless Communications and Networking, vol.2004, no.11, pp.19–31, 2006.

[51] J. Liu, F. Fsu, and J. Yee, Control PHY design for 40–50 GHz millimeter wave communication systems, IEEE 802.11-15/0705, 2015.

[52] F. Hsu, J. Yee, and J. Liu, Bandwidth and packet type detection schemes for 40–50 GHz millimeter wave communication, IEEE 802.11-15/0706, 2015.

[53] H. Wang, W. Hong, J. Zhu, S. He, et al., Channel generation of 802.11aj (45 GHz) based on channel measurement, IEEE 802.11-14/0721r1, 2014.

[54] H. Wang, Channel model description and channel generation for IEEE 802.11aj (45 GHz), IEEE 802.11-14/0893r0, 2014.

Appendix

The OSTF sequence is given by

$$\frac{1+j}{\sqrt{2}}\{0, \boldsymbol{a}, \boldsymbol{a}, \boldsymbol{b}, \boldsymbol{a}, \boldsymbol{a}, \boldsymbol{a}, \boldsymbol{b}, \boldsymbol{b}, \boldsymbol{a}, \boldsymbol{b}, \boldsymbol{b}, \boldsymbol{b}, \boldsymbol{a}, \boldsymbol{a}, \boldsymbol{b}, \boldsymbol{a}, \boldsymbol{b}, \boldsymbol{b}, \boldsymbol{a}, \boldsymbol{b}, \boldsymbol{a},$$
$$\boldsymbol{a}, 0, 0, 0, 0, \boldsymbol{b}, \boldsymbol{b}, \boldsymbol{b}, \boldsymbol{b}, \boldsymbol{a}, \boldsymbol{b}, \boldsymbol{b}, \boldsymbol{b}, \boldsymbol{a}, \boldsymbol{a}, \boldsymbol{a}, \boldsymbol{a}, \boldsymbol{b}, \boldsymbol{a}, \boldsymbol{a}, \boldsymbol{a}, \boldsymbol{b}, \boldsymbol{a}, \boldsymbol{b}, \boldsymbol{a},$$
$$\boldsymbol{a}, 0, 0\}$$

for 540 MHz channel where $\boldsymbol{a} = [1, 0, 0, 0]$ and $\boldsymbol{b} = [-1, 0, 0, 0]$, and

$$\frac{1+j}{\sqrt{2}}\{0, \boldsymbol{b}, \boldsymbol{a}, \boldsymbol{a}, \boldsymbol{a}, \boldsymbol{b}, \boldsymbol{b}, \boldsymbol{b}, \boldsymbol{a}, \boldsymbol{a}, \boldsymbol{b}, \boldsymbol{a}, \boldsymbol{a}, \boldsymbol{a}, \boldsymbol{a}, \boldsymbol{b}, \boldsymbol{b}, \boldsymbol{b}, \boldsymbol{b}, \boldsymbol{a}, \boldsymbol{b}, \boldsymbol{a},$$
$$\boldsymbol{b}, \boldsymbol{b}, \boldsymbol{b}, \boldsymbol{a}, \boldsymbol{b}, \boldsymbol{b}, \boldsymbol{a}, \boldsymbol{b}, \boldsymbol{a}, \boldsymbol{b}, \boldsymbol{a}, \boldsymbol{a}, \boldsymbol{b}, \boldsymbol{b}, \boldsymbol{a}, \boldsymbol{a}, \boldsymbol{b}, \boldsymbol{a}, \boldsymbol{a}, \boldsymbol{a}, \boldsymbol{b}, \boldsymbol{a}, \boldsymbol{b}, 0, 0,$$
$$0, 0, \boldsymbol{a}, \boldsymbol{a}, \boldsymbol{b}, \boldsymbol{b}, \boldsymbol{b}, \boldsymbol{b}, \boldsymbol{b}, \boldsymbol{b}, \boldsymbol{b}, \boldsymbol{a}, \boldsymbol{a}, \boldsymbol{b}, \boldsymbol{b}, \boldsymbol{a}, \boldsymbol{a}, \boldsymbol{a}, \boldsymbol{a}, \boldsymbol{a}, \boldsymbol{a}, \boldsymbol{b}, \boldsymbol{a}, \boldsymbol{a}, \boldsymbol{a},$$
$$\boldsymbol{a}, \boldsymbol{a}, \boldsymbol{b}, \boldsymbol{a}, \boldsymbol{a}, \boldsymbol{a}, \boldsymbol{b}, \boldsymbol{a}, \boldsymbol{b}, \boldsymbol{a}, \boldsymbol{a}, \boldsymbol{a}, \boldsymbol{a}, \boldsymbol{a}, \boldsymbol{a}, \boldsymbol{a}, \boldsymbol{a}, \boldsymbol{a}, \boldsymbol{b}, \boldsymbol{b}, -1, 0\}$$

for 1080 MHz channel. For 540 MHz channel, the value on the subcarrier with the index from −89 to 89 of the OCEF field is given by

$$1, -1, -1, 1, 1, -1, -1, 1, 1, -1, 1, 1, 1, 1, 1, 1, 1, 1, -1, -1, 1,$$
$$-1, 1, 1, 1, -1, 1, 1, -1, 1, -1, -1, 1, 1, -1, -1, 1, -1, 1, 1, 1, 1,$$
$$1, 1, 1, -1, -1, 1, 1, 1, -1, 1, 1, -1, 1, -1, 1, -1, -1, -1, 1, -1,$$
$$-1, -1, -1, 1, 1, -1, -1, -1, -1, -1, -1, 1, -1, -1, -1, 1, 1, 1,$$
$$1, -1, -1, 1, 1, -1, 1, 1, 0, 0, 0, -1, 1, -1, 1, 1, -1, 1, -1, -1,$$
$$-1, 1, 1, 1, 1, 1, -1, -1, -1, 1, 1, 1, 1, -1, -1, -1, -1, -1, -1,$$
$$-1, 1, -1, 1, -1, 1, 1, 1, -1, -1, -1, -1, 1, 1, -1, -1, -1, 1, 1,$$
$$-1, 1, 1, -1, 1, 1, 1, 1, -1, 1, -1, -1, -1, 1, -1, 1, -1, 1, -1, 1,$$
$$-1, 1, 1, 1, 1, -1, 1, -1, 1, -1, -1, 1, 1, 1, -1, 1, 1, -1, -1, -1, 1.$$

For 1080 MHz channel, the value on the subcarrier with the index from −177 to 177 of the OCEF field is given by

$$1, -1, 1, -1, -1, -1, -1, -1, 1, 1, -1, -1, 1, 1, 1, 1, 1, -1, -1,$$
$$-1, -1, 1, -1, 1, -1, 1, 1, 1, 1, -1, 1, 1, -1, -1, 1, 1, 1, -1, 1, 1,$$
$$-1, -1, 1, -1, -1, -1, 1, -1, 1, 1, -1, 1, 1, 1, -1, -1, 1, -1, -1,$$
$$-1, -1, -1, 1, 1, -1, -1, -1, -1, -1, 1, -1, 1, 1, 1, -1, -1, -1,$$
$$-1, 1, 1, 1, -1, 1, 1, 1, 1, -1, -1, 1, 1, -1, 1, 1, 0, 0, 0, 1, 1, 1,$$
$$-1, -1, -1, 1, -1, 1, 1, -1, 1, 1, -1, 1, 1, -1, 1, -1, 1, 1, 1, 1,$$
$$-1, 1, 1, -1, 1, -1, 1, 1, 1, 1, 1, 1, -1, -1, 1, -1, -1, -1, 1, -1,$$
$$1, 1, -1, 1, 1, 1, -1, -1, 1, -1, 1, 1, 1, 1, -1, 1, 1, 1, -1, 1, 1, 1,$$
$$1, -1, 1, -1, -1, -1, 1, -1, 1, 1, 1, -1, -1, -1, -1, -1, -1, 1.$$

Wei Hong received the B.S. degree from the University of Information Engineering, Zhengzhou, China, in 1982, and the M.S. and Ph.D. degrees from Southeast University, Nanjing, China, in 1985 and 1988, respectively, all in radio engineering. Since 1988, he has been with the State Key Laboratory of Millimeter Waves and serves for the director of the lab since 2003, and is currently a professor and the dean of the School of Information Science and Engineering, Southeast University. In 1993, 1995, 1996, 1997 and 1998, he was a short-term Visiting Scholar with the University of California at Berkeley and at Santa Cruz, respectively. He has been engaged in numerical methods for electromagnetic problems, millimeter wave theory and technology, antennas, RF technology for wireless communications etc. He has authored and co-authored over 300 technical publications with over 9000 citations, and authored two books. He twice awarded the National Natural Prizes, thrice awarded the first-class Science and Technology Progress Prizes issued by the Ministry of Education of China and Jiangsu Province Government etc. Besides, he also received the Foundations for China Distinguished Young Investigators and for 'Innovation Group' issued by NSF of China. Dr. Hong is a Fellow of IEEE, Fellow of CIE, the vice presidents of the CIE Microwave Society and Antenna Society, the Chair of the IEEE MTT-S/AP-S/EMC-S Joint Nanjing Chapter, and was an elected IEEE MTT-S AdCom Member during 2014–2016. He served as the Associate Editor of the IEEE Trans. on MTT from 2007 to 2010, one of the Guest editors for the 5G special issue of IEEE Trans. on AP in 2017.

Shiwen He was born in 1978. He received the M.S. degree from Chengdu University of Technology, Chengdu, China, and the Ph.D. degree in information and communication engineering from Southeast University, Nanjing, China, in 2009 and 2013, respectively. From 2013 to 2015, he was a Postdoctoral Researcher with the State Key Laboratory of Millimeter Waves, Department of Radio Engineering, Southeast University. Since October 2015, he has been with the School of Information Science and Engineering, Southeast University. He has authored or coauthored over 80 technical publications, hold over 16 granted invention patents, and submitted over 20 technical proposals to IEEE standards. From December 2015, he serves as a technical sub-editor for IEEE 802.11aj. His research interests include multiuser MIMO communication, cooperative communications, energy efficient communications, millimeter wave communication, and optimization theory.

Haiming Wang was born in 1975. He received the M.S. and Ph.D. degrees in electrical engineering from Southeast University, Nanjing, China, in 2002 and 2009, respectively. He joined the State Key Laboratory of Millimeter Waves, Southeast University, in April 2002. Now he is an Associate Professor. His current research interests include radio propagation measurement and channel modelling, signal processing for MIMO wireless communications, and millimeter-wave wireless communications. Dr. Wang received the first-class Science and Technology Progress Award of Jiangsu Province of China in 2009. He is currently serves as the vice chair of IEEE 802.11aj task group.

Guangqi Yang received his B.S. degree in electronic engineering from Nanjing University of Aeronautics and Astronautics, China, in 1995 and M.Sc. degree in electronic engineering from Southeast University, China, in 2002. From then on, he has been worked with Southeast University and focused on techniques, tools and platforms for design and implementation of large-scale prototypes which support verification and demonstration of innovative RF and millimeter applications. His current research interests concern joint design of RF and baseband systems, high level synthesis, algorithm parallelizing and continuous integration technologies for FPGA-centric development.

Yongming Huang received the B.S. and M.S. degrees from Nanjing University, Nanjing, China, in 2000 and 2003, respectively, and the Ph.D. degree in electrical engineering from Southeast University, Nanjing, in 2007. Since March 2007, he has been a faculty member with the School of Information Science and Engineering, Southeast University, China, where he is currently a full professor. In 2008–2009, he visited the Signal Processing Laboratory, School of Electrical Engineering, Royal Institute of Technology (KTH), Stockholm, Sweden. His current research interests include MIMO wireless communications, cooperative wireless communications and millimeter wave wireless communications. He has published over 200 peer-reviewed papers, hold over 40 invention patents, and submitted over 10 technical contributions to IEEE standards. Since 2012, he has served as an Associate Editor for the IEEE Transactions on Signal Processing, EURASIP Journal on Advances in Signal Processing, and EURASIP Journal on Wireless Communications and Networking. He was elected as the Changjiang Young Scholar of Ministry of Education of China in 2015.

Jixin Chen was born in Jiangsu Province, P.R. China, in 1976. He received the B.S. degree in radio engineering from Southeast University, Nanjing, China, in 1998, and the M.S. and Ph.D. degrees from Southeast University, Nanjing, China, in 2002 and 2006, respectively, all in electromagnetic field and microwave technique. Since 1998, he has been with the Sate Key Lab. of Millimeter Waves, Southeast University, and is currently professor of School of Information Science and Engineering. His current research interests include microwave and millimeter-wave circuit design and MMIC design. He has authored and co-authored more than 100 papers and presented invited papers at ICMMT2016, IMWS2012, GSMM2011. He is the winner of 2016 Keysight Early Career Professor Award. He has served as TPC co-chair of HSIC2012, UCMMT2012, LOC co-chair of APMC2015, session co-chair of iWAT2011, ISSSE2010, APMC2007, and reviewer for IEEE MTT and IEEE MWCL.

Jianyi Zhou received the B.S. degree, the M.S. degree and the Ph.D. degrees from Southeast University, Nanjing, China, in 1989, 1996 and 2001, respectively, all in radio engineering. Since 1996, he has been with the State Key Laboratory of Millimeter Waves, Southeast University. His research focuses on the RF techniques and systems for the wireless communication systems. The developed RF systems have been used in many communication systems, such as the first MIMO system in China, the B3G tri-networks in China, the first Gbps mobile communication system in China, the first wideband MIMO mobile communication tri-network in the high frequency band in China, the RoF networks for the IMT-Advanced systems, the next generation WLAN systems, the massive MIMO systems for the 5G mobile communications, etc. His researches on the nonlinear RF circuits were reported in IEEE Transaction on Microwave Theory and Techniques, and have been used in many RF systems. He developed several efficient absorbing boundary conditions for the finite-difference time-domain method. Currently, he is engaged in the development of RF systems for the 5G mobile communications and millimeter wave communications.

Xiaowei Zhu received the M.E. and Ph.D. degrees in radio engineering from Southeast University, Nanjing, China in 1996 and 2000, respectively. Since 1984, he has been with Southeast University, where he is currently a Professor with the School of Information Science and Engineering. He has authored or coauthored over 90 technical publications. He holds 15 patents. His research interests include RF and antenna technologies for wireless communications, as well as microwave and millimeter-wave theory and technology, and also power amplifier (PA) nonlinear character and its linearization research with a particular emphasis on wideband and high-efficiency GaN PAs. Dr. Zhu is president of the Microwave Integrated Circuits and Mobile Communication Sub-Society, the Microwave Society of CIE, and the secretary of the IEEE MTT-S/AP-S/EMC-S Joint Nanjing Chapter. He was the recipient of the 1994 First-Class Science and Technology Progress Prize presented by the Ministry of Education of China and the 2003 Second-Class Science and Technology Progress Prize of Jiangsu Province, China.

Nianzu Zhang received the M.S. and Ph.D. degrees from Southeast University in 2003 and 2012, respectively. His research interests include wireless channel measurement and emulation; channel modelling and simulation; massive MIMO system for 5G Mobile Communications. He has applied for or published more than 10 patents, authored and co-authored more than 20 journal and conference publications.

Jianfeng Zhai received the B.S.E.E. and Ph.D. degrees from Southeast University, Nanjing, China, in 2004 and 2009, respectively. In 2009, he joined the faculty of the School of Information Science and Engineering, Southeast University, as a Lecturer, and became an Associate Professor in 2013. His current research interests include digital signal processing, nonlinear modeling, microwave circuits design, power amplifier linearization.

Luxi Yang received the M.S. and Ph.D. degree in electrical engineering from the Southeast University, Nanjing, China, in 1990 and 1993, respectively. Since 1993, he has been with the Department of Radio Engineering, Southeast University, where he is currently a full professor of information systems and communications, and the Director of Digital Signal Processing Division. His current research interests include signal processing for wireless communications, MIMO communications, cooperative relaying systems, and statistical signal processing. He has authored or co-authored of two published books and more than 100 journal papers, and holds 30 patents. Prof. Yang received the first and second class prizes of science and technology progress awards of the state education ministry of China in 1998, 2002 and 2014. He is currently a member of Signal Processing Committee of Chinese Institute of Electronics.

Zhihao Jiang was born in Nanjing, China, in 1986. He received the B.S. degree in radio engineering from Southeast University, Nanjing, China, in 2008, and Ph.D. in electrical engineering from The Pennsylvania State University, in 2013. He is currently a Full Professor with the State Key Laboratory of Millimeter Waves, School of Information Science and Engineering, Southeast University, Nanjing, China. From August 2013 to July 2016, he was a postdoc fellow at the Computational Electromagnetics and Antennas Research Lab (CEARL) in the Department of Electrical Engineering at The Pennsylvania State University, USA. From July 2007 to August 2007, he was an intern at the Base Station Antenna R&D, Andrew Telecommunication (China). His research interests include antennas, transmit-arrays, impedance surfaces, microwave circuits, metamaterials, and nanophotonics. Dr. Jiang holds 3 US patents (granted) and 1 Chinese patent (granted), has authored over 90 papers in peer reviewed international journals and conference proceedings, as well as 7 book chapters. He has co-edited 1 book: Electromagnetics of Body-area Networks: Antennas, Propagation, and RF Systems (Wiley/IEEE Press, 2016). He is the recipient of the Thousands of Young Talents presented by China government in 2016, the Honorable Mention in 2013 IEEE AP-S International Symposium on Antennas and Propagation Student Paper Contest, the 2012 A. J. Ferraro Outstanding Doctoral Research Award in Electromagnetics, the 2007 Microsoft Young Fellow awarded by Microsoft Research Asia (MSRA), and the Meritorious Winner of the 2006 Interdisciplinary Contest in Modeling funded by National Security Agency and administrated by the Consortium for Mathematics and its Applications. He is a Member of IEEE. He also serves as a reviewer for Nature Communications, Scientific Reports, IEEE Transactions on Antennas and Propagation, IEEE Transactions on Biomedical Circuits and Systems, IEEE Antennas and Wireless Propagation Letters, IEEE Microwave and Wireless Component Letters, IEEE Antennas and Propagation Magazine, Applied Physics Letters, and so on.

Chao Yu was born in 1984. He received the Ph.D. degree in electronic engineering from University College Dublin, Dublin, Ireland, in 2014. He is currently an associate professor with the State Key Laboratory of Millimeter Waves, School of Information Science and Engineering, Southeast University. His research interests include microwave and millimeter wave power amplifier modeling and linearization,and 5G wireless system design.